Structure of the Antimicrobial Peptide Tritrpticin Bound to Micelles: A Distinct Membrane-Bound Peptide Fold[†,‡]

David J. Schibli, Peter M. Hwang, and Hans J. Vogel*

Department of Biological Sciences, University of Calgary, Calgary, Alberta T2N 1N4, Canada

Received March 25, 1999; Revised Manuscript Received October 20, 1999

ABSTRACT: Tritrpticin is a member of the cathelicidin family, a group of diverse antimicrobial peptides found in neutrophil granules. The three Trp and four Arg residues in the sequence VRRFPWWWPFLRR make this a Trp-rich cationic peptide. The structure of tritrpticin bound to membrane-mimetic sodium dodecyl sulfate micelles has been determined using conventional two-dimensional NMR methods. It forms two adjacent turns around the two Pro residues, a distinct fold for peptide−membrane interaction. The first turn involves residues 4−7, followed immediately by a second well-defined 3_{10}-helical turn involving residues 8−11. The hydrophobic residues are clustered together and are clearly separated from the basic Arg residues, resulting in an amphipathic structure. Favorable interactions between the unusual amphipathic fold and the micelle surface are probably key to determining the peptide structure. NMR studies of the peptide in the micelle in the presence of the spin-label 5-doxylstearic acid determined that tritrpticin lies near the surface of the micelle, where its many aromatic side chains appear to be equally partitioned into the hydrophilic−hydrophobic interface. Additional fluorescence studies confirmed that the tryptophan residues are inserted into the micelle and are partially protected from the effects of the soluble fluorescence quencher acrylamide.

Antimicrobial peptides are an integral part of the nonspecific immune defense system (*1*). They are frequently secreted onto epithelial surfaces or released by neutrophils at sites of inflammation (*2*), thus limiting the growth and survival of potentially pathogenic microorganisms. These cationic peptides are found in all living organisms, including insects, bacteria, and vertebrates (*3*). To combat the increasing emergence of drug-resistant bacteria (*4*), antimicrobial peptides have become a potential source of new antibiotics (*5*).

One major class of antimicrobial peptides is the cathelicidins, mammalian antimicrobial peptides synthesized in the granules of myeloid cells (*6*). Cathelicidins are expressed as preproproteins. The 29−30-residue "pre" sequence directs the protein for secretion. The next 100 N-terminal amino acids constitute the "pro" region, a conserved sequence homologous to porcine cathelin. Cathelin is homologous to the cystatin family of cysteine protease inhibitors, but the function of this domain remains uncertain. The cathelin domain contains many acidic residues, and it may serve to keep the basic antimicrobial peptide in an inactive state prior to secretion (*7*). The active antimicrobial domain follows the pro region. Upon cleavage by an elastase-like protease, the cathelin-like domain is removed to yield an active antimicrobial peptide (*8*).

While the pro region is homologous to cathelin, the C-terminal antimicrobial peptides have highly variable sequences (*6*). Cathelicidins have been identified in cows (*9*), pigs (*10*), rabbits (*11*), sheep (*12*), mice (*13*), and humans (*14*). Cathelicidins can have very diverse amino acid compositions and secondary structures. Many are α-helical, such as CRAMP (*13*) and CAP18 (*11*). A few, such as the protegrins, are *β*-sheets (*15*). Other cathelicidins are rich in Pro and Arg residues, so regular secondary structures are unlikely. Of these, a fragment of Bac5 has been shown to adopt a type II polyproline helix (*16*).

Tritrpticin is a cathelicidin with a high proportion of Trp residues. It is a 13-amino acid peptide with the sequence VRRFPWWWPFLRR (*17*). The presence of three consecutive Trp residues is unique for antimicrobial peptides, while the presence of two Pro and four Arg residues resembles the composition of a class of Arg/Pro-rich cathelicidins (*6*). The sequence was identified as the longest stretch of amphipathic residues in a potential porcine cathelicidin cDNA, containing a cathelin-like domain. This sequence is actually only the first part of a longer 100-amino acid sequence which contains five Pro- and Phe-rich decamer repeats (*10*). The 79 C-terminal residues that make up these tandem repeats have been isolated as an intact peptide, named prophenin-1, from porcine leukocytes (*18*).

While the tritrpticin peptide has yet to be isolated from porcine neutrophils, the synthetic tritrpticin peptide was found to have potent broad spectrum antibacterial as well as antifungal activities (*17*). Like many antimicrobial peptides, it is probable that tritrpticin exerts its microbicidal effect at the bacterial cell membrane. It is thought that these peptides will bind to microbial membranes and cause disruption of the membrane leading to lysis (*3*). Membrane-active peptides

[†] This work was supported by an operating grant from the Medical Research Council of Canada. P.M.H. and H.J.V. hold a Studentship and Scientist Award, respectively, from the Alberta Heritage Foundation for Medical Research. D.J.S. holds a Province of Alberta Graduate Fellowship.

[‡] Coordinates have been deposited in the Protein Data Bank (file name 1D6X).

* To whom correspondence should be addressed. Telephone: (403) 220-6006. Fax: (403) 289-9311. E-mail: vogel@ucalgary.ca.

10.1021/bi990701c CCC: $18.00
Published on Web 12/03/1999

are often unstructured in solution and require a polar−nonpolar interface to form their correct membrane-active structure. The use of micelles (rather than phospholipid bilayers) is necessary for high-resolution solution state nuclear magnetic resonance (NMR)[1] in determining peptide structure, due to the increase in the rotational correlation time of larger macromolecules (*19*−*21*).

In this work, we have determined the structure of tritrpticin bound to membrane-mimetic sodium dodecyl sulfate (SDS) micelles by conventional 2D NMR methods. This study aids in the elucidation of the mechanism of lysis of microbial membranes and demonstrates the structural characteristics that are important for tritrpticin's interactions with membranes. The NMR structure of tritrpticin reveals a distinct structural fold, brought about by protein−membrane interaction.

EXPERIMENTAL PROCEDURES

Materials. Tritrpticin was synthesized by the Peptide Synthesis Facility at Queen's University and purified using reverse phase HPLC (University of Waterloo, Waterloo, ON). The purity was assessed by mass spectrometry. Perdeuterated SDS and D_2O were purchased from Cambridge Isotope Laboratories, Inc. Nitroxide spin-labeled fatty acids were purchased from Sigma.

CD Spectroscopy. CD measurements were taken on a Jasco J-715 CD spectrophotometer with a 1 mm path length cylindrical cuvette. Wavelengths from 185 to 255 nm were measured, with a 0.2 nm step resolution, a 50 nm/min speed, a 2 s response time, and a 1 nm bandwidth. Spectra were collected and averaged over eight scans. Samples (10 μM) of tritrpticin were prepared in 10 mM Tris (pH 7.0). SDS was added to a concentration of 35 mM for the tritrpticin−SDS sample. The SDS background was subtracted from CD spectra acquired for the peptide.

NMR Spectroscopy. All NMR spectra were acquired on a Bruker AMX500 spectrometer. A 3 mM sample of tritrpticin was prepared in 9:1 H_2O/D_2O and the pH adjusted to 4.5. The concentration was confirmed by measuring the UV absorption of a diluted sample and assuming a calculated molar extinction coefficient (at 280 nm) of 16 500 M^{-1} cm^{-1}. 1D ^1H spectra were recorded at 16, 25, and 37 °C. Perdeuterated SDS (400 mM) was added to the sample, and 1D ^1H spectra were recorded at 25, 37, and 40 °C. DQF-COSY (*22*), TOCSY (*23*) (mixing time 60 ms), and NOESY (*24*) (100 ms mixing time) spectra were acquired at 40 °C. A NOESY experiment in the presence of 5-doxylstearic acid was performed by adding spin-labeled stearic acid from a 0.1 M stock solution in deuterated methanol to obtain a final ratio of SDS to spin-label of 60:1 (*25*). Water suppression was achieved using low-power presaturation during the relaxation delay. In addition, a z-gradient pulse was applied at the end of the mixing time in the NOESY experiment. The number of data points in the F_2 and F_1 dimensions was 2048 and 512, respectively, with a spectral width of 6024 Hz. The spectra were zero-filled to a 2K × 2K matrix. The data were processed on a Silicon Graphics Indy workstation using NMRPIPE (*26*).

To study amide exchange rates, the previous NMR sample was lyophilized and redissolved in 99.9% D_2O and 1D spectra were recorded as soon as possible. Spectra were acquired after 5, 20, and 40 min and 24 h.

Structure Calculations. Distance restraints were obtained from the NOESY spectra using NMRVIEW 3.1 (*27*). On the basis of NOE peak volumes, distance restraints were classified as strong, medium, and weak corresponding to upper boundaries of 2.8, 3.3, and 5.0 Å, respectively. Pseudoatom corrections were also applied to degenerate and nonstereospecifically assigned protons. The ϕ dihedral angle was constrained between −35° and −180° (usually the only range considered in NMR-derived structures).

Structures were calculated with a single round of restrained simulated annealing molecular dynamics using CNS (*28*). The starting structure went through a high-temperature annealing stage and two slow-cooling annealing stages using the default settings of CNS. The force field used constrained the geometry (i.e., bond lengths, angles, and improper angles), maintained van der Waals distances, and constrained the molecule to satisfy distance and dihedral restraints. The structure was then subjected to 200 steps of Powell energy minimization. Of the 100 structures that were generated, the 18 lowest-energy structures were kept, which did not have bond violations of >0.05 Å and angle violations of >5.0°.

Fluorescence Spectroscopy. Tryptophan fluorescence was monitored on a Hitachi F-2000 fluorimeter, with an excitation wavelength of 295 nm and the emission scanned from 300 to 450 nm. Scans were taken with a 10 nm excitation and emission bandwidth and a scan speed of 60 nm/s. The concentration of tritrpticin samples was 2 μM, in 10 mM Tris (pH 7.2) and 10 mM NaCl and in the presence or absence of 25 mM SDS. For fluorescence quenching experiments, acrylamide was added from a 4 M stock solution to final concentrations between 0.01 and 0.6 M. The quenched samples were excited at 295 nm, and the emission was monitored at the peak maximum determined from the wavelength scan in the absence of quencher. The effect of the acrylamide on the fluorescence of the peptide was analyzed using the quenching constant (K_{SV}) as determined by the Stern−Volmer equation (*29*).

RESULTS

CD Spectroscopy. The CD spectra of tritrpticin recorded with and without SDS are shown in Figure 1. It is evident that a structural change is induced upon binding of the peptide to the SDS micelles. The negative peak at 225 nm becomes more prominent, while the large negative peak at 185 nm disappears and is replaced by a positive peak at 196 nm.

Interpretation of the tritrpticin CD spectra is complicated by the presence of multiple aromatic side chains, preventing a detailed analysis of secondary structure. For instance, the tryptophan side chain contributes to CD spectra around 200 and 220 nm (*30*). Tritrpticin has a very large negative ellipticity at 185 nm when it is free in solution, typical for a random coil structure. Upon addition of SDS, this negative ellipticity disappears, suggesting a more ordered structure.

[1] Abbreviations: NMR, nuclear magnetic resonance; SDS, sodium dodecyl sulfate; CD, circular dichroism; DSS, sodium 3-(trimethylsilyl)-1-propanesulfonate; NOE, nuclear Overhauser effect; DQF-COSY, double-quantum-filtered correlation spectroscopy; NOESY, nuclear Overhauser enhancement spectroscopy; TOCSY, total correlation spectroscopy; 1D, one-dimensional; 2D, two-dimensional.

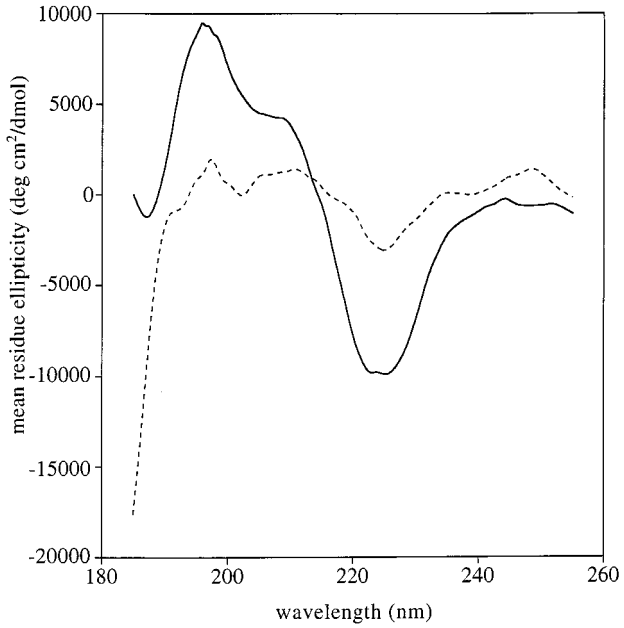

FIGURE 1: CD spectra taken on a Jasco J-715 CD spectrometer with 10 μM tritrpticin in 10 mM Tris at pH 7 and 25 °C in the absence (dashed) and presence (solid) of 35 mM SDS.

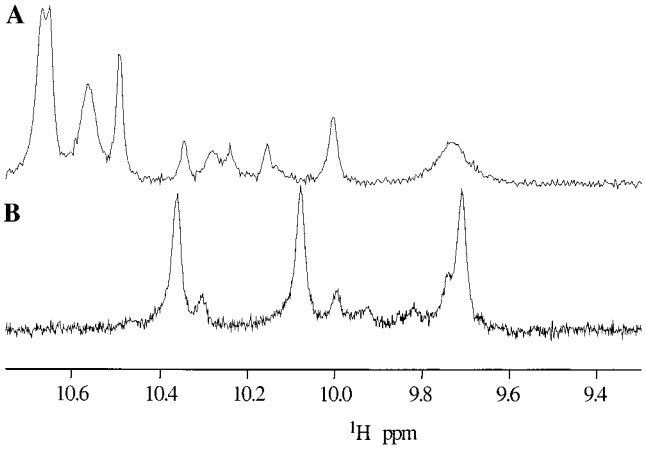

FIGURE 2: Downfield chemical shift region of the 1D ^{1}H NMR spectrum of 3 mM tritrpticin at pH 4.5 and 25 °C in 9:1 H_2O/D_2O (A) without SDS and (B) with SDS.

Addition of SDS also results in a negative peak around 225 nm, which could be caused by either the tryptophan side chains (*30*) or turn structures (*31*). In tritrpticin, both features probably contribute.

NMR Spectroscopy. For peptides, the region of the 1D ^{1}H spectrum between 9.5 and 11 ppm contains mainly tryptophan indole NH signals. Since there are three tryptophans in tritrpticin, this region would be expected to contain three peaks. However, there are approximately 12 peaks in this region, as seen in Figure 2A. These likely correspond to the three indole NH signals; however, they appear as 12 peaks because there are four slowly interconverting conformations of tritrpticin. Cis−trans isomerization of its two proline residues would produce four conformations: trans−trans, cis−trans, trans−cis, and cis−cis. Upon addition of SDS, the 12 Trp peaks shown in trace A collapsed into three major peaks, as shown in trace B, suggesting the formation of a single stable conformer. Still, at least one minor conformer is evident. However, its signals were sufficiently weak that it did not interfere with chemical shift assignments or NOESY cross-peak compilation. 1D spectra of tritrpticin−SDS were better resolved at 40 °C than at 25 °C, so further spectra were acquired at high temperatures.

Chemical shift assignments for tritrpticin were made according to the method of Wüthrich (*32*). All of the protons of Pro5 and Pro9, as well as the β-protons of Trp6 and Phe10, were stereospecifically assigned, on the basis of NOE cross-peaks. The amide resonance for Arg12 was only observed in the TOCSY spectrum and hence is not labeled in the NOESY spectra (Figure 3). There were a number of unusual chemical shifts observed. For example, the amide proton of Trp7 appeared at 6.13 ppm. Many side chain resonances were also shifted upfield considerably, e.g., the βH of Pro5 at 0.57 and 1.59 ppm. The anomalous chemical shifts are likely due to multiple ring current shifts induced by the many aromatic rings contained in tritrpticin. Additionally, it is also possible that the negative charge of the SDS molecules could affect the chemical shifts.

Proton NMR spectra of tritrpticin−SDS were recorded at various time intervals after being dissolved in D_2O (at 40 °C). The amides belonging to residues 4−11 could be observed after 20 min. It may be that the exchange rates for some amides were slowed slightly due to burying within the micelle (*33*). After 40 min, only the amides of Trp7, Trp8, and Leu11 remained. The amide of Phe4 is possibly also present, but its chemical shift overlaps with Leu11. After 24 h, all the amide protons had been exchanged. However, no hydrogen bonds were included in the structure calculations, and some of these residues appeared in a hydrogen-bonded conformation in the calculated structures (see below).

Solution Structure of Tritrpticin. Altogether, there were 163 interproton restraints used in the structure calculations derived from the NOESY spectrum (Figure 3). Of these, 47 were intraresidue, 50 sequential, and 66 medium-range. Restraints that would not constrain protons further than geometric restraints (e.g., between protons in the same aromatic ring or within a proline residue) were not included. We also added 12 broad dihedral angle restraints (see Experimental Procedures).

Most of the medium-range restraints that were identified were between hydrophobic residues, located from position 4 to 11. Few NOESY peaks were observed between Val1 and the other hydrophobic residues. Some cross-peaks were observed for Arg2-Arg3 and Arg12-Arg13, but could not be resolved due to spectral overlap. Consequently, the NMR structures converged well for residues 4−11, but not for the N- and C-termini. The overall rmsd for the family of 18 final structures was 1.62 Å for backbone atoms and 3.27 Å for heavy atoms. If only residues 4−11 were considered, the rmsd was 0.28 Å for backbone atoms and 0.77 Å for heavy atoms (see Table 1).

Tritrpticin adopts a double-turn structure (Figure 4A,C). The first turn is comprised of Phe4-Pro5-Trp6-Trp7. The program Molmol (*34*, *59*) does not assign any hydrogen-bonded partners in the first turn of the calculated tritrpticin structure. This could suggest that hydrogen bonding does not occur in this region; however, the overall geometry approaches that of a type IV turn. The failure to clearly identify the hydrogen bonding in the first turn probably arises from the lack of two to three crucial backbone NOEs for this region in the structural calculations. These are probably present, but they could not be assigned unequivocally because

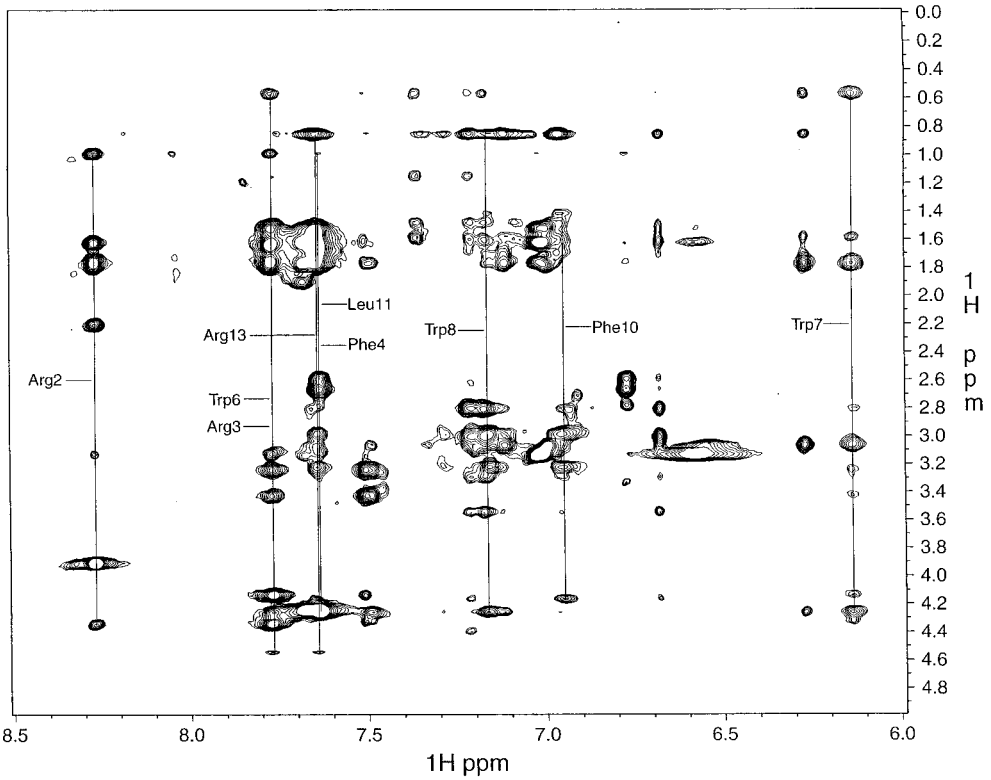

FIGURE 3: Fingerprint region of the NOESY spectrum for 3 mM tritrpticin in 9:1 H_2O/D_2O and 400 mM SDS-d_{25} at pH 4.5 and 40 °C with a mixing time of 100 ms. All of the amide resonances are labeled, except for Arg12 which only appeared in the TOCSY spectrum.

Table 1: Summary of Structural Statistics for Tritrpticin in SDS Micelles

total no. of distance constraints	163
no. of intraresidue constraints	47
no. of sequential constraints ($\|i-j\|=1$)	50
no. of medium-range constraints ($1<\|i-j\|\leq 4$)	66
total no. of dihedral constraints	
ϕ	12
rms deviations form experimental constraints	
distance constraints (Å)	0.030 ± 0.0019
dihedral constraints (deg)	0.11 ± 0.090
rms deviations from ideal geometry	
covalent bonds (Å)	0.0036 ± 0.00016
covalent angles (deg)	0.5526 ± 0.0088
impropers (deg)	0.25 ± 0.011
average pairwise atomic rms differences[a]	
backbone (Å)	1.62 ± 0.51 (0.28 ± 0.15)
heavy atoms (Å)	3.27 ± 0.81 (0.77 ± 0.23)

[a] The values for residues 1−13 (residues 4−11 are in parentheses).

of extensive peak overlap in this region. However, it is well-known that hydrogen bond formation is favored in peptides bound to a membrane interface (*35*); moreover, some of the amide resonances in this region exchange more slowly, suggesting that hydrogen bonding does occur. The second turn immediately follows the first and consists of Trp8-Pro9-Phe10-Leu11, forming a type III turn (3_{10}-helix). The amide group of Leu11 is hydrogen bonded to the carbonyl oxygen of Trp8 in at least half of the computed structures as indicated by Molmol (*34*, *59*). We also observed the characteristic NOE pattern for this turn, involving residues 8−11. It is also possible that the amide of Trp8 forms an additional hydrogen bond in this turn, because of its slower amide exchange characteristics. Pro5 and Pro9 are both in the trans conformation. The structure of tritrpticin brings all of the hydrophobic side chains except Val1 together into a single patch (Figure 4B). A remarkable feature of the structure is the clustering of aromatic and aliphatic amino acid side chains, a structure that bears some similarity to the hydrophobic core of a soluble protein. The N- and C-terminal ends are not well-resolved in the family of NMR structures. However, even though the terminal Arg residues are not resolved, they seem to be oriented on the side opposite the hydrophobic cluster in all of the NMR-derived solution structures, yielding an amphipathic structure (Figure 4B).

Interactions between Tritrpticin and the Micelle. 5-Doxyl-stearic acid was added to a tritrpticin−SDS NMR sample in a 1:60 spin-label:detergent ratio, approximately one spin-label per micelle (*25*). A NOESY spectrum revealed that the signals corresponding to the side chains of Phe4, Trp6, Trp7, Trp8, Phe10, and Leu11 were broadened considerably. The side chains of all Arg residues, as well as Val1, were not significantly broadened. This is consistent with the structural model of tritrpticin, bound on the surface of the SDS micelle so that the hydrophobic patch faces the center of the micelle, while the other residues are oriented more superficially (*36*). Val1 was not part of the main hydrophobic surface in the structural model, and it may not be able to partition deeply into the micelles due to its positively charged amino terminus. The Val1 residue was not essential for antimicrobial activity (*17*), and it is likely that it is cleaved off with the pro region of the protein (*10*).

Tryptophan Fluorescence. The presence of tritrpticin in the SDS micelles was confirmed by determining the effect of SDS micelles on the tryptophan fluorescence emission spectra. The addition of SDS micelles to the peptide sample caused a 7 nm blue shift in the emission peak from 349 to

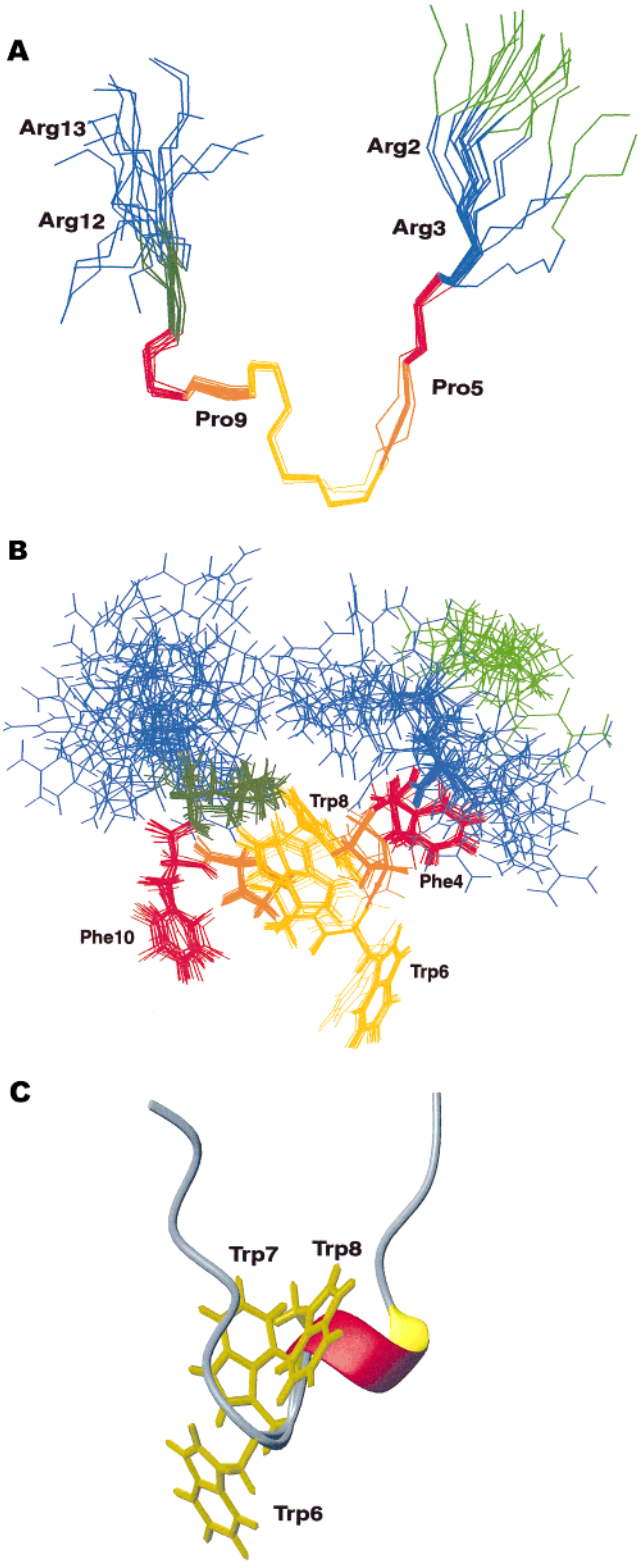

FIGURE 4: (A) Backbone (Cα, N, and C) atoms of the 18 final structures of tritrpticin bound to SDS. Residues 4−11 are overlayed. The Arg residues are blue, the Phe residues red, the Pro residues orange, the Trp residues gold, the Leu residue is dark green and the Val residue light green. (B) All atoms in the 18 final structures of tritrpticin bound to SDS. Residues 4−11 are overlayed. (C) Ribbon diagram of the average structure of tritrpticin. The side chains of Trp6, Trp7, and Trp8 are visible (gold). These figures were made with Molmol (*34*, *59*).

342 nm (Figure 5A). This blue shift is representative of the Trp residue being partitioned into a more hydrophobic

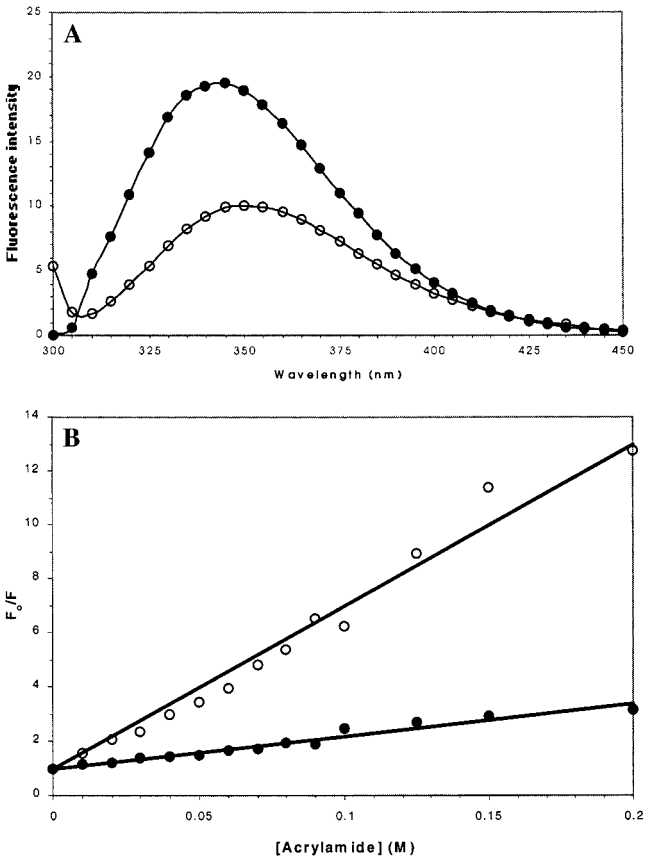

FIGURE 5: (A) Fluorescence emission spectrum and (B) Stern−Volmer plot of 2 μM tritrpticin in the absence (○) and presence (●) of SDS micelles at 25 °C. Stern−Volmer plots were obtained by the sequential addition of small volumes of the fluorescence quencher acrylamide.

environment (*37*), which would be expected if the Trp residues were positioned among the acyl chains of the SDS molecules. It was also observed that the fluorescence intensity of the Trp residues increased from approximately 12 to 20 fluorescence units (Figure 5A), suggesting that the Trp residues were more sterically confined (*37*).

To determine the extent to which the Trp residues are sequestered in the hydrophobic core of the micelle, a fluorescence quenching experiment was performed using acrylamide. Due to the incidence of static quenching at higher acrylamide concentrations (*29*), the K_{SV} constants were calculated from the plots between 0 and 0.2 M acrylamide. The Stern−Volmer constants (K_{SV}) for tritrpticin were 59 and 11 M^{-1} in the absence and presence of the SDS micelle, respectively (Figure 5B). These values confirm that when the peptide is free in solution, it is much more accessible to the quencher than when in the presence of the micelles. The protection of the Trp residues by the micelle from the water soluble acrylamide confirms that they are partially buried in the hydrophobic core of the micelle.

DISCUSSION

Most membrane protein structures elucidated to date have regular α-helical or β-sheet secondary structures (*38*). As such, the formation of backbone hydrogen bonds is very energetically favorable in membrane interfaces (*39*). Also, a cationic amphipathic structure would be best suited for maximizing both electrostatic and hydrophobic interactions

with a membrane. However, for the partial tritrpticin sequence, FPWWWPFL, a conventional α-helix or β-sheet would be unable to place all of the hydrophobic side chains onto one side. To allow for hydrophobic grouping, the unusual two-turn fold of tritrpticin does contain some hydrogen bonds, but not as many as would be found in a conventional secondary structure. It appears that the folding of tritrpticin is dominated by interactions between amino acid side chains and the SDS micelle. Additionally, the formation of the turn−turn structure of tritrpticin is presumably stabilized by the two aromatic residues flanking each of the Pro residues, as in the well-documented type VI turn (*40*). It is interesting to note that similar cysteine-stabilized turns have been found to be the primary structural element of the lantibiotic nisin (*36*), although these cause five separate amphipathic ring structures to form.

The tri-Trp sequence of tritrpticin appears to be a hydrophobic insert into the Pro/Arg-rich region which is continued in the subsequent peptide prophenin-1 (*18*). In the structure of tritrpticin, the Trp (Figure 4C) and Phe residues are placed into a single hydrophobic surface where they can interact favorably with the hydrophobic−hydrophilic membrane interface. This is likely the impetus for the formation of tritrpticin's two-turn fold. Aromatic side chains, particularly the indole ring of tryptophan, strongly prefer partitioning into the interfacial region of membranes (*35*, *41*, *42*). Indole and other Trp analogues have recently been found to be located near the carbons closest to the glycerol headgroup of POPC lipids (*43*, *44*). This confirms the previous results of Kachel et al. (*45*), which showed that carbazole, a Trp analogue, is found at the polar−hydrocarbon interface.

Preliminary CD, fluorescence, and NMR studies (data not shown) with the related Trp-rich bovine neutrophil 13-residue antimicrobial peptide, indolicidin (*46*), suggest that it may interact with SDS micelles in a manner comparable to that of tritrpticin and adopt a similar but more flexible turn-like structure upon binding to SDS micelles. While this paper was under review, a CD and modeling study of indolicidin in membrane-mimetic environments was published; this work also suggested the presence of turns in the membrane-bound indolicidin structure (*47*). In addition, we have recently described the structure of the antimicrobial center of lactoferricin B in SDS micelles (*48*), an amidated hexapeptide that contains two Trp and three Arg residues that possesses the majority of the antimicrobial activity of lactoferricin B (*49*). This short peptide does not form a standard secondary structure, but does form a stable amphipathic structure with the Trp residues buried in the micelle and the Arg residues on opposite sides of the structure. The clustering of the aromatic residues and the separation of the hydrophobic and basic residues is similar to the overall tertiary structure that was observed here for tritrpticin. The importance of tryptophan for membrane interactions seen for these three Trp-rich peptides has also been observed in other membrane-active peptides that possess Trp residues, such as galanin (*25*), gramicidin A (*50*), and mellitin (*51*).

The presence and orientation of tritrpticin in the SDS micelle were confirmed by both NMR spin-label broadening studies and fluorescence spectroscopy. It is difficult to estimate an actual depth for the peptide in the micelle from these experiments since the doxyl spin-label will broaden the proton resonances from a large distance (*52*). This position in a micelle would likely integrate it into the plane of a lipid bilayer. The partial burial of the Trp residues was confirmed by the increased protection of their fluorescence from the quenching of acrylamide when in the presence of SDS micelles. It would be possible in principle to determine the depth of tritrpticin in the micelles by fluorescence quenching using the parallax method (*53*); unfortunately, the presence of multiple Trp residues in tritrpticin complicates these calculations.

While the aromatic residues of tritrpticin apparently cause the peptide to be inserted into membranes, the basic residues will stabilize this interaction by interacting with the negatively charge micelle surface and probably aid in the selectivity of the peptide for microbial membranes (*54*−*56*). The well-studied antimicrobial peptide magainin-2 has been found to cause positive-curvature strain in various phospholipid vesicles, with pore formation being strongly dependent on the lipid composition of the vesicle (*57*). There is preliminary evidence that tritrpticin may cause disruption of membranes by inducing positive-curvature strain in model membranes in the same fashion as magainin-2 (personal communication from R. Epand, Hamilton, ON). Additionally, electron microscopy studies of the effect of tritrpticin on bacterial membranes suggest that the peptide acts directly on the inner and outer membranes (personal communication from T. Mietzner, Pittsburgh, PA).

In this study, we have determined the solution structure of the antimicrobial peptide tritrpticin in membrane-mimetic SDS micelles. The micelle-bound peptide has a turn−turn structure. It was found that the peptide forms a marked amphipathic structure in SDS with the hydrophobic aromatic residue positioned deeper in the micelle. Most antimicrobial peptides form such amphipathic structures (*58*). The high tryptophan and phenylalanine content of this peptide and the burial of these residues in the micelle suggest that they play a critical role in the antimicrobial activity of this peptide. Future studies on the interactions of mutants of this peptide with phospholipid bilayers, and the effect of altering the tryptophan content on its activity, may lead to a better understanding of the role of tryptophan in the lytic mechanism of this and other Trp-rich antimicrobial peptides.

SUPPORTING INFORMATION AVAILABLE

An NOE summary for tritrpticin and the ^{1}H chemical shift assignment, as well as a Ramachandran diagram for the calculated structures. This material is available free of charge via the Internet at http://pubs.acs.org.

REFERENCES

1. Boman, H. G. (1995) *Annu. Rev. Immunol. 13*, 61−92.
2. Ganz, T., and Lehrer, R. I. (1998) *Curr. Opin. Immunol. 10*, 41−44.
3. Hancock, R. E. W., Falla, T., and Brown, M. (1995) *Adv. Microb. Rev. 37*, 135−175.
4. Davies, J. (1994) *Science 264*, 375−382.
5. Hancock, R. E. W. (1997) *Clin. Infect. Dis. 24* (Suppl. 1), 148−150.
6. Zanetti, M., Gennaro, R., and Romeo, D. (1995) *FEBS Lett. 374*, 1−5.
7. Storici, P., Tossi, A., Lenarcic, B., and Romeo, D. (1996) *Eur. J. Biochem. 238*, 769−776.
8. Panyutich, A., Shi, J., Boutz, P. L., Zhao, C., and Ganz, T. (1997) *Infect. Immun. 65*, 978−985.

9. Scocchi, M., Wang, S., and Zanetti, M. (1997) *FEBS Lett. 417*, 311−315.
10. Pungercar, J., Strukelj, B., Kopitar, G., Renko, M., Lenarcic, B., Gubensek, F., and Turk, V. (1993) *FEBS Lett. 336*, 284−288.
11. Chen, C., Brock, R., Luh, F., Chou, P.-J., Larrick, J. W., Huang, R.-F., and Huang, T.-H. (1995) *FEBS Lett. 370*, 46−52.
12. Huttner, K. M., Lambeth, M. R., Burkin, H. R., Burkin, D. J., and Broad, T. E. (1998) *Gene 206*, 85−91.
13. Gallo, R. L., Kim, K. J., Bernfield, M., Kozak, C. A., Zanetti, M., Merluzzi, L., and Gennaro, R. (1997) *J. Biol. Chem. 272*, 13088−13093.
14. Agerberth, B., Gunne, H., Odeberg, J., Kogner, P., Boman, H. G., and Gudmundsson, G. H. (1995) *Proc. Natl. Acad. Sci. U.S.A. 92*, 195−199.
15. Roumestand, C., Louis, V., Aumelas, A., Grassy, G., Calas, B., and Chavanieu, A. (1998) *FEBS Lett. 421*, 263−267.
16. Raj, P. A., Marcus, E., and Edgerton, M. (1996) *Biochemistry 35*, 4314−4325.
17. Lawyer, C., Pai, S., Watabe, M., Borgia, P., Mashimo, T., Eagleton, L., and Watabe, K. (1996) *FEBS Lett. 390*, 95−98.
18. Harwig, S. S. L., Kokryakov, V. N., Swiderek, K. M., Aleshina, G. M., Zhao, C., and Lehrer, R. I. (1995) *FEBS Lett. 362*, 65−69.
19. Henry, G. D., and Sykes, B. D. (1994) *Methods Enzymol. 239*, 515−535.
20. MacKenzie, K. R., Prestegard, J. H., and Engelman, D. M. (1997) *Science 276*, 131−133.
21. Opella, S. J. (1997) *Nat. Struct. Biol. 4* (Suppl.), 845−848.
22. Rance, M., Sorenson, O. W., Bodenhausen, G., Wagner, G., Ernst, R. R., and Wüthrich, K. (1983) *Biochem. Biophys. Res. Commun. 117*, 479−495.
23. Braunschweiller, L., and Ernst, R. R. (1983) *J. Magn. Reson. 53*, 521−528.
24. Jeener, J., Meier, B. H., Bachmann, P., and Ernst, R. R. (1979) *J. Chem. Phys. 71*, 4546−4553.
25. Ohman, A., Lycksell, P. O., Jureus, A., Langel, U., Bartfai, T., and Graslund, A. (1998) *Biochemistry 37*, 9169−9178.
26. Delaglio, F., Grzesiek, S., Vuister, G. W., Zhu, G., Pfeifer, J., and Bax, A. (1995) *J. Biomol. NMR 6*, 277−293.
27. Johnson, B. A., and Blevins, R. A. (1994) *J. Biomol. NMR 4*, 603−614.
28. Brunger, A. T., Adams, P. D., Clore, G. M., DeLano, W. L., Gros, P., Grosse-Kunstleve, R. W., Jiang, J. S., Kuszewski, J., Nilges, M., Pannu, N. S., Read, R. J., Rice, L. M., Simonson, T., and Warren, G. L. (1998) *Acta Crystallogr. D54*, 905−921.
29. Eftink, M. R., and Ghiron, C. A. (1976) *J. Phys. Chem. 80*, 486−493.
30. Woody, R. W. (1994) *Eur. Biophys. J. 23*, 253−262.
31. Yang. J. J., Pitkeathly, M., and Radford, S. E. (1994) *Biochemistry 33*, 7345−7353.
32. Wüthrich, K. (1986) *NMR of Proteins and Nucleic Acids*, John Wiley and Sons, New York.
33. Spyracopoulos, L., and O'Neil, J. D. J. (1994) *J. Am. Chem. Soc. 116*, 1395−1402.
34. Koradi, R., Billeter, M., and Wuthrich, K. (1996) *J. Mol. Graphics 14*, 51−55.
35. Wimley, W. C., and White, S. J. (1996) *Nat. Struct. Biol. 3*, 842−848.
36. Van den Hooven, H. W., Spronk, C. A. E. M., Van de Kamp, M., Konings, R. N. H., Hilbers, C. W., and Van de Ven, F. J. M. (1996) *Eur. J. Biochem. 235*, 394−403.
37. Campbell, I. D., and Dwek, R. A. (1984) *Biological Spectroscopy*, pp 91−125, Benjamin/Cummings, Menlo Park, CA.
38. Walker, J. E., and Saraste, M. (1996) *Curr. Opin. Struct. Biol. 6*, 457−459.
39. Ladokhin, A. S., and White, S. H. (1999) *J. Mol. Biol. 285*, 1363−1369.
40. Yao, J., Dyson, H. J., and Wright, P. E. (1994) *J. Mol. Biol. 243*, 754−766.
41. Hu, W., Lee, K. C., and Cross, T. A. (1993) *Biochemistry 32*, 7035−7047.
42. Reithmeier, R. A. F. (1995) *Curr. Opin. Struct. Biol. 5*, 491−500.
43. Yau, W.-M., Wimley, W. C., Gawrisch, K., and White, S. H. (1998) *Biochemistry 37*, 14713−14718.
44. Persson, S., Killian, J. A., and Lindblom, G. (1998) *Biophys. J. 75*, 1365−1371.
45. Kachel, K., Asuncion-Punzalan, E., and London, E. (1995) *Biochemistry 34*, 15475−15479.
46. Selsted, M. E., Novotny, M. J., Morris, W. L., Tang, Y. Q., Smith, W., and Cullen, J. S. (1992) *J. Biol. Chem. 267*, 4292−4295.
47. Ladokhin, A. S., Selsted, M. E., and White, S. H. (1999) *Biochemistry* (in press).
48. Schibli, D. J., Hwang, P. M., and Vogel, H. J. (1999) *FEBS Lett. 446*, 213−217.
49. Tomita, M., Takase, M., Bellamy, W., and Shimamura, S. (1994) *Acta Paediatr. Jpn. 36*, 585−591.
50. Kethcem, R. R., Hu, W., and Cross, T. A. (1993) *Science 261*, 1457−1460.
51. Blondelle, S. E., and Houghten, R. A. (1991) *Pept. Res. 4*, 12−18.
52. Dwek, R. H. (1973) *Nuclear Magnetic Resonance in Biochemistry: Applications to Enzyme Systems*, Clarenden Press, Oxford, U.K.
53. Chattopadhyay, A., and London, E. (1987) *Biochemistry 26*, 39−45.
54. Liu, L.-P., and Deber, C. M. (1997) *Biochemistry 36*, 5476−5482.
55. Polozov, I. V., Polozova, A. I., Tytler, E. M., Anantharamaiah, G. M., Segrest, J. P., Woolley, G. A., and Epand, R. M. (1997) *Biochemistry 36*, 9237−9245.
56. Breukink, E., van Kraaij, C., van Dalen, A., Demel, R. A., Siezen, R. J., de Kruijff, B., and Kuipers, O. P. (1998) *Biochemistry 37*, 8153.
57. Matsuzaki, K., Sugishita, K., Ishibe, N., Ueha, M., Nakata, S., Miyajima, K., and Epand, R. M. (1998) *Biochemistry 37*, 11856−11863.
58. Hwang, P. M., and Vogel, H. J. (1998) *Biochem. Cell Biol. 76*, 235−246.
59. Koradi, R., Billeter, M., and Wuthrich, K. (1996) *J. Mol. Graphics 14*, 29−32.

BI990701C